Acta Crystallographica Section F
Structural Biology Communications
ISSN 2053-230X

Expression, purification, crystallization and preliminary X-ray crystallographic analysis of Enpp6

Junko Morita,[a] Kazuki Kato,[a] Emiko Mihara,[b] Ryuichiro Ishitani,[a] Junichi Takagi,[b] Hiroshi Nishimasu,[a] Junken Aoki[c] and Osamu Nureki[a]*

[a]Department of Biological Science, Graduate School of Science, The University of Tokyo, 2-11-16 Yayoi, Bunkyo-ku, Tokyo 113-0032, Japan, [b]Institute for Protein Research, Osaka University, 3-2 Yamadaoka, Suita, Osaka 565-0871, Japan, and [c]Graduate School of Pharmaceutical Sciences, Tohoku University, 6-3 Aoba, Aramaki, Aoba-ku, Sendai, Miyagi 980-8578, Japan

Correspondence e-mail: nureki@bs.s.u-tokyo.ac.jp

Received 18 March 2014
Accepted 19 April 2014

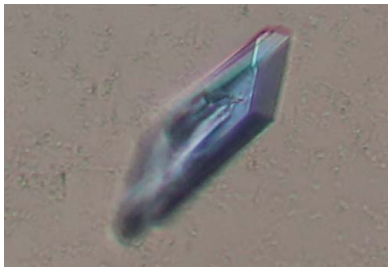

© 2014 International Union of Crystallography
All rights reserved

Enpp (ectonucleotide phosphodiesterase/pyrophosphatase) 6 is a membrane-bound glycoprotein that hydrolyzes choline-containing compounds such as lysophosphatidylcholine and glycerophosphorylcholine, and presumably participates in choline metabolism. The catalytic domain of mouse Enpp6 was expressed in HEK293T cells, purified using the TARGET tag/P20.1-Sepharose system and crystallized. An X-ray diffraction data set was collected to 1.8 Å resolution. The crystal belonged to space group $P1$, with unit-cell parameters a = 63.7, b = 68.8, c = 69.7 Å, α = 60.6, β = 87.0, γ = 68.1°. Assuming the presence of two protein molecules per asymmetric unit, the solvent content was estimated to be 49.5%.

1. Introduction

Enpp (ectonucleotide phosphodiesterase/pyrophosphatase) family proteins are extracellular enzymes that hydrolyze phosphodiester or pyrophosphate bonds in various compounds (Stefan *et al.*, 2005). They are conserved in vertebrates, and mammals have seven family members (Enpp1–Enpp7). Enpp1–Enpp3 are multidomain proteins consisting of two somatomedin B-like domains, a catalytic domain and a nuclease-like domain, whereas Enpp4–Enpp7 have only a catalytic domain. Although they share a similar catalytic domain, the Enpp family members show distinct substrate specificities and participate in various cellular processes. Enpp1 hydrolyzes extracellular nucleotide triphosphates to produce pyrophosphate and regulates bone mineralization (Hessle *et al.*, 2002). In contrast, Enpp2 hydrolyzes lysophosphatidylcholine (LPC) to produce lysophosphatidic acid (LPA), which activates G-protein-coupled receptors to induce various cellular responses (Umezu-Goto *et al.*, 2002). Recent studies have shown that Enpp3 hydrolyzes UDP-GlcNAc to generate UMP and regulates the synthesis of N-linked and *O*-mannosyl glycans (Korekane *et al.*, 2013), whereas Enpp4 hydrolyzes the dinucleotide adenosine(5′)triphospho(5′)adenosine and is involved in haemostasis and platelet aggregation (Albright *et al.*, 2012). The crystal structures of Enpp1, Enpp2 and Enpp4 revealed that the insertion loop in the catalytic domain is a major determinant of the substrate specificities of the Enpp family proteins (Hausmann *et al.*, 2011; Nishimasu *et al.*, 2011; Jansen *et al.*, 2012; Kato, Nishimasu, Okudaira *et al.*, 2012; Albright *et al.*, 2013). Enpp1 and Enpp4 have a nucleotide-binding pocket formed by the insertion loop (Kato, Nishimasu, Okudaira *et al.*, 2012; Albright *et al.*, 2013), whereas Enpp2 has an LCP-binding hydrophobic pocket, since it lacks the insertion loop (Nishimasu *et al.*, 2011).

Enpp6 is expressed in the kidney, brain and liver, and is bound to the plasma membrane through its C-terminal glycosylphosphatidylinositol (GPI) anchor (Sakagami *et al.*, 2005; Greiner-Tollersrud *et al.*, 2013). Enpp6 hydrolyzes choline-containing extracellular compounds, such as LPC and glycerophosphocholine (GPC), *in vitro*. These observations suggested that Enpp6 is involved in choline metabolism, although its physiological roles remain elusive. Enpp6 hydrolyzes LPC to generate phosphocholine and monoacylglycerol (lysoPLC activity), whereas Enpp2 hydrolyzes LPC to generate LPA and choline (lysoPLD activity). This catalytic difference suggested that whereas Enpp2 has a hydrophobic pocket that

accommodates the acyl chains of LPC substrates (Nishimasu *et al.*, 2011), Enpp6 has an active-site pocket that recognizes the choline head group of LPC substrates. However, the choline-recognition mechanism of Enpp6 remains unknown because of a lack of structural information.

2. Materials and methods

2.1. Construction

We constructed an expression plasmid encoding the catalytic domain (residues 1–421) of mouse Enpp6 fused with the C-terminal TARGET tag, which consists of 21 amino acids (YPGQ×5 + V) and is recognized by the P20.1 antibody (Tabata *et al.*, 2010). DNA fragments encoding the catalytic domain of mouse Enpp6 were PCR-amplified by PrimeSTAR MAX DNA polymerase (TaKaRa) using pCAG-GS-Enpp6 as the template. The PCR products were inserted into the *Xba*I and *Kpn*I sites of pcDNA3.1 (Invitrogen), which had been modified to contain a C-terminal *Tobacco etch virus* (TEV) protease cleavage site followed by the TARGET tag (referred to as pcD-CW; Tabata *et al.*, 2010). The expression vectors encoding Enpp6 mutants were prepared by site-directed mutagenesis using pcD-CW-Enpp6 as the template. The sequences were verified by DNA sequencing.

2.2. Protein preparation

The wild type and mutants of Enpp6 were expressed as secreted forms in stably transfected HEK293S GnT1$^-$ cells or transiently transfected HEK293T cells. The cells were cultured in DMEM medium (Sigma) supplemented with 10%(*v*/*v*) FBS (Euro Clone), 1%(*v*/*v*) MEM non-essential amino acids (Sigma) and 1%(*v*/*v*) sodium pyruvate (Gibco) and were incubated at 310 K in a humidified atmosphere containing 5% CO_2. HEK293S GnT1$^-$ cells were co-transfected with the expression plasmid and the IR/MAR plasmid (Trans Genic Inc.) using the Lipofectamine 2000 reagent (Invitrogen). Stably transfected cell lines were established in medium containing 1 mg ml^{-1} G418 (Nacalai Tesque) and 100 µg ml^{-1} Blasticidin (InvivoGen), and were cloned by a limiting-dilution procedure in 96-well plates for two weeks. To obtain a single clone secreting a high level of Enpp6, we evaluated the clones by measuring the phosphodiesterase activity in culture supernatants using *p*-nitrophenylphosphorylcholine as a substrate, as described by Sakagami *et al.* (2005). HEK293T cells were transfected with the expression plasmid, using the Lipofectamine 2000 reagent, and were then cultured on 150 mm dishes for 3 d.

The wild type and mutants of Enpp6 were purified from the culture supernatants using P20.1-Sepharose resin and a Superdex 200 Increase gel-filtration column (GE Healthcare) in essentially the same manner as described for Enpp1 (Kato, Nishimasu, Mihara *et al.*, 2012). The TARGET tag was cleaved by TEV protease before the gel-filtration step. For crystallization, the C393A/C412S mutant was purified using the P20.1-Sepharose resin followed by TARGET tag cleavage. The protein was further purified by chromatography on a HiLoad 16/60 Superdex 200 gel-filtration column (GE Healthcare), concentrated to 2 mg ml^{-1} using an Amicon Ultra-4 filter (10 kDa

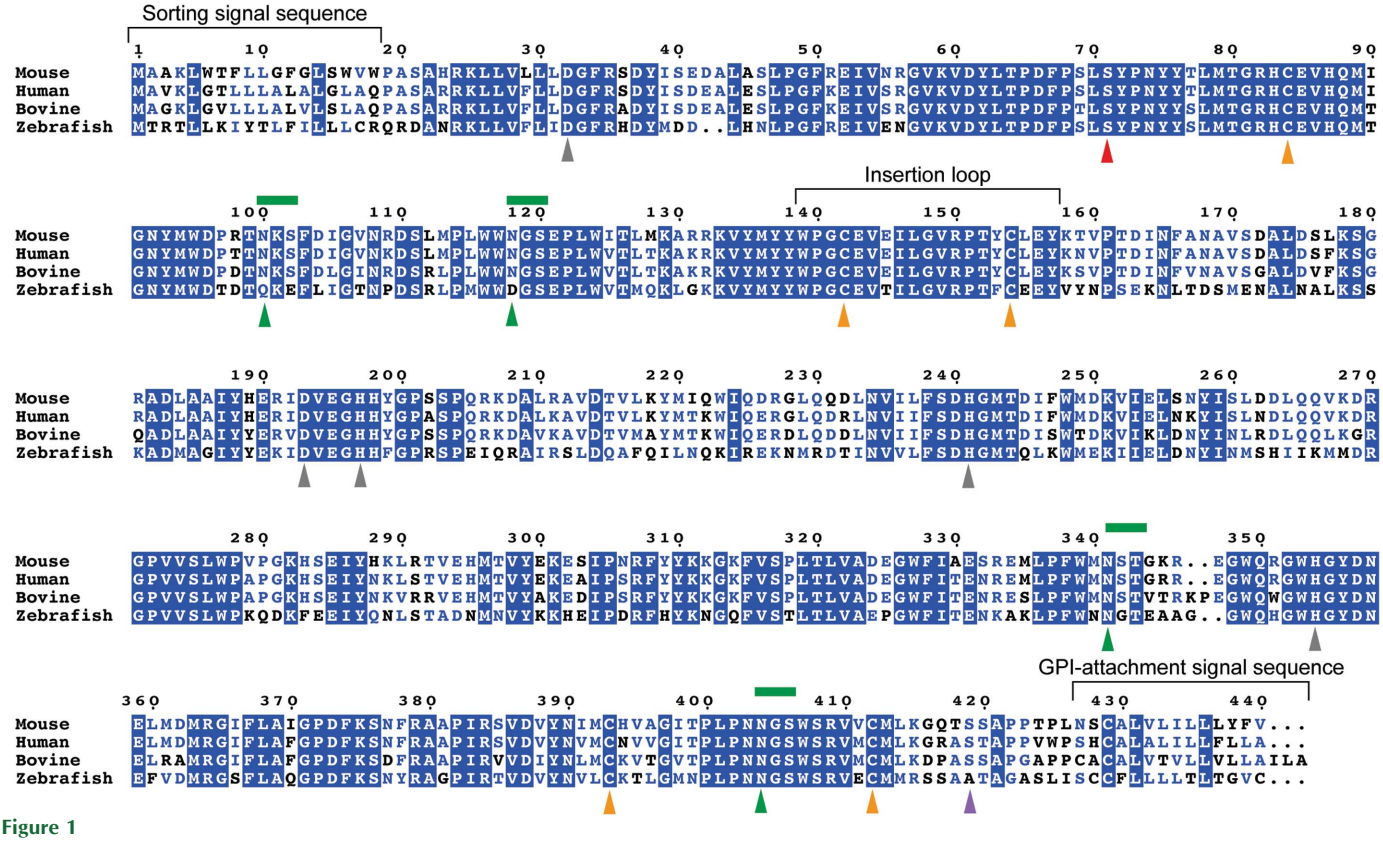

Figure 1
Multiple sequence alignment of Enpp6. The catalytic residue and the zinc-coordinating residues are indicated by red and grey triangles, respectively. The conserved cysteine residues are indicated by orange triangles. The putative N-glycosylated asparagine residues and the consensus sequences for N-glycosylation are indicated by green triangles and green lines, respectively. The predicted C-terminal GPI-attachment residue is indicated by a purple triangle. The sequence alignment was prepared using *ClustalW* (Larkin *et al.*, 2007) and *ESPript* (Gouet *et al.*, 2003).

molecular-weight cutoff; Millipore) and then stored at 193 K until use. The purity and oligomeric state of the protein were assessed by SDS–PAGE in the presence (reducing conditions) and absence (nonreducing conditions) of 5% β-mercaptoethanol, and the gels were stained with Simply Blue SafeStain (Invitrogen).

2.3. Crystallization

Initial crystallization screening was performed at 293 K by the sitting-drop vapour-diffusion method in an MRC 96-well Crystallization Plate (Molecular Dimensions) using the following screening kits: Crystal Screen (Hampton Research), The PACT Suite and The JCSG+ Suite (Qiagen) and JBScreen Classic 1, 2, 4 and 5 (Jena Bioscience). Crystallization droplets were prepared by mixing 100 nl protein solution (2 mg ml^{-1} Enpp6 in 20 m*M* Tris–HCl pH 7.5, 150 m*M* sodium chloride, 0.2 m*M* zinc sulfate, 10 m*M* phosphocholine) and 100 nl reservoir solution using a Mosquito crystallization robot (TTP Labtech). Initial hits were optimized at 293 K by the sitting-drop vapour-diffusion method by mixing 200 nl protein solution and 200 nl reservoir solution.

2.4. Data collection and preliminary crystallographic analysis

Crystals were cryoprotected in reservoir solution supplemented with 25%(*v*/*v*) ethylene glycol and were flash-cooled in liquid nitrogen. X-ray diffraction experiments were performed on beamline PXI at the Swiss Light Source, Villigen, Switzerland using a Pilatus 6M detector. A data set was collected at a wavelength of 1.278 Å with an oscillation angle of 360° (0.1° per frame), an exposure time of 0.1 s per frame and a transmission of 10%. Diffraction images were integrated and scaled using *XDS* (Kabsch, 2010). Molecular replacement was performed with *MOLREP* (Vagin & Teplyakov, 2010), using the catalytic domain (residues 190–579) of mouse Enpp1 (PDB entry 4gtw; Kato, Nishimasu, Okudaira *et al.*, 2012) as a search model.

3. Results and discussion

3.1. Protein preparation

Since we successfully expressed Enpp1 (Kato, Nishimasu, Mihara *et al.*, 2012) and Enpp2 (Nishimasu *et al.*, 2011) in HEK293S GnT1$^-$ cells as soluble secreted proteins, we expressed the catalytic domain

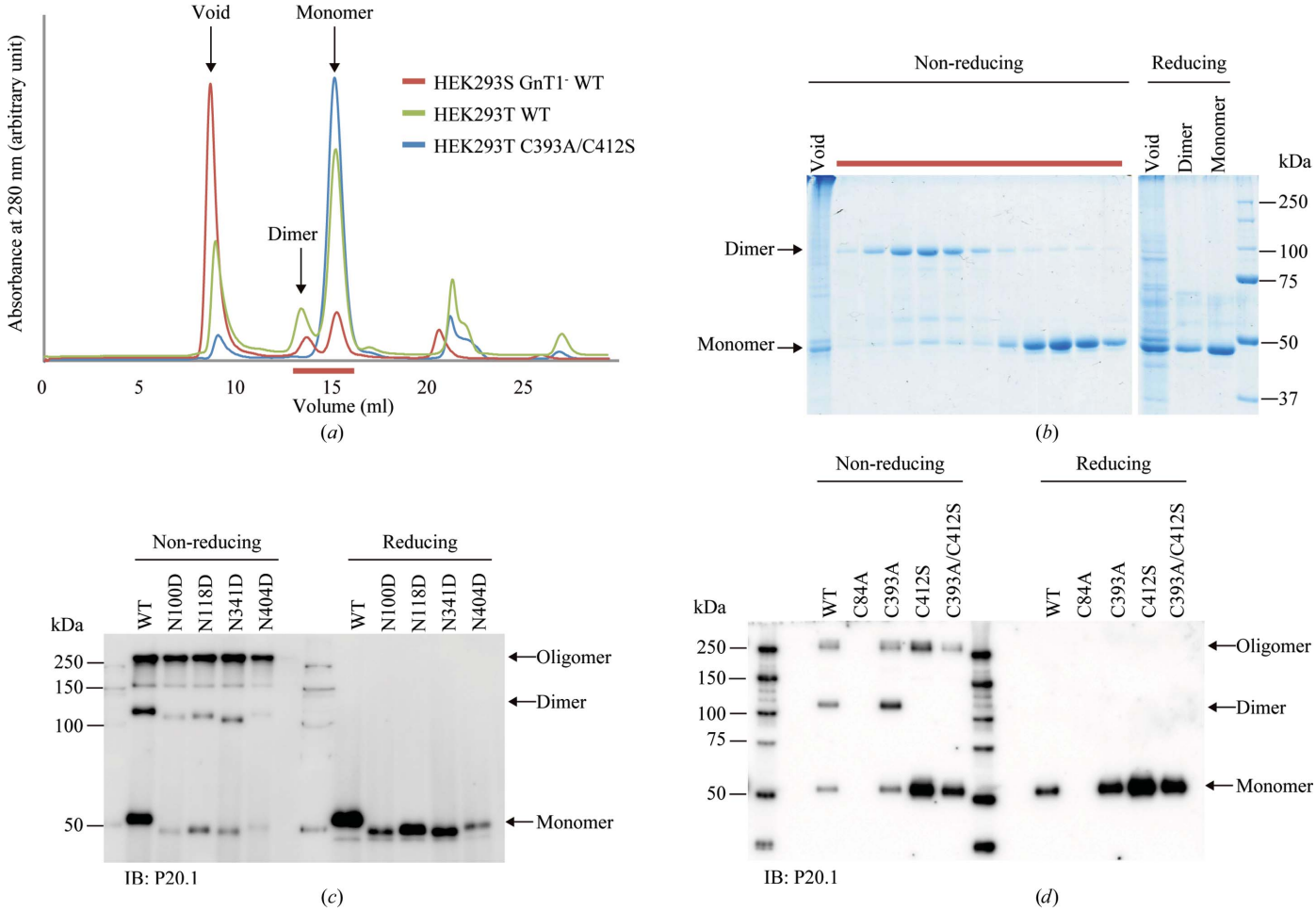

Figure 2
Oligomeric state of the wild type and mutants of Enpp6. (*a*) Gel-filtration analysis of wild-type Enpp6 expressed in HEK293S GnT1$^-$ cells and the wild type and C393A/C412S mutant of Enpp6 expressed in HEK293T cells. The proteins were purified by P20.1-Sepharose and then chromatographed on a Superdex 200 Increase gel-filtration column. WT, wild type. (*b*) SDS–PAGE analysis of wild-type Enpp6 expressed in HEK293S GnT1$^-$ cells. The fractions indicated by the red line in (*a*) were analyzed by SDS–PAGE under reducing and nonreducing conditions. (*c*) Effect of N-glycosylation on the oligomeric state of Enpp6. The wild type and N-glycosylation site mutants of Enpp6 were expressed in HEK293T cells, purified by P20.1-Sepharose and analyzed by SDS–PAGE under reducing and nonreducing conditions. The proteins were detected by the P20.1 antibody. (*d*) Effect of the cysteine residues on the oligomeric state of Enpp6. The wild type and cysteine mutants of Enpp6 were expressed, purified and then analyzed as in (*c*). The C84A mutant was not expressed in HEK293T cells.

(residues 1–421) of Enpp6, which lacks the C-terminal GPI-anchor signal sequences (residues 422–440), in HEK293S GnT1$^-$ cells (Fig. 1). However, unlike Enpp1 and Ennp2, the affinity-purified Enpp6 protein predominantly eluted in the void volume from the gel-filtration column, with two small peaks corresponding to molecular weights of 50 and 100 kDa (Fig. 2*a*). Reducing and nonreducing SDS–PAGE analyses revealed that these three peaks are all composed of Enpp6, indicating that Enpp6 exists as a mixture of monomers, dimers and higher-order oligomers in solution (Fig. 2*b*). In addition, these results indicated that the observed oligomerization is mediated by intermolecular disulfide linkages. In contrast, when Enpp6 was expressed in HEK293T cells, the monomeric population of Enpp6 eluted from the gel-filtration column increased remarkably, with a concomitant decrease in the dimeric and higher-order oligomeric populations (Fig. 2*a*). Given that HEK293S GnT1$^-$ and HEK293T cells produce proteins with high mannose N-linked glycans and complex N-linked glycans, respectively (de Vries *et al.*, 2010), these observations indicated that complex N-linked glycosylation is important for preventing the disulfide-mediated oligomerization of Enpp6.

Enpp6 has four predicted consensus sequences for N-glycosylation [N*X*(S/T), where *X* is any amino-acid residue other than Pro; Fig. 1], and a mass-spectrometric analysis confirmed that the four N-glycosylation sites are indeed modified in bovine Enpp6 (Greiner-Tollersrud *et al.*, 2013). To examine the effects of N-glycosylation on the oligomeric state of Enpp6, we prepared the four mutants of mouse Enpp6 (N100D, N118D, N341D and N404D). Western blotting analysis revealed that the monomeric populations of the four mutants were remarkably reduced compared with that of the wild type (Fig. 2*c*), indicating that all four of the N-glycosylation modifications are important for preventing the disulfide-mediated oligomerization of Enpp6.

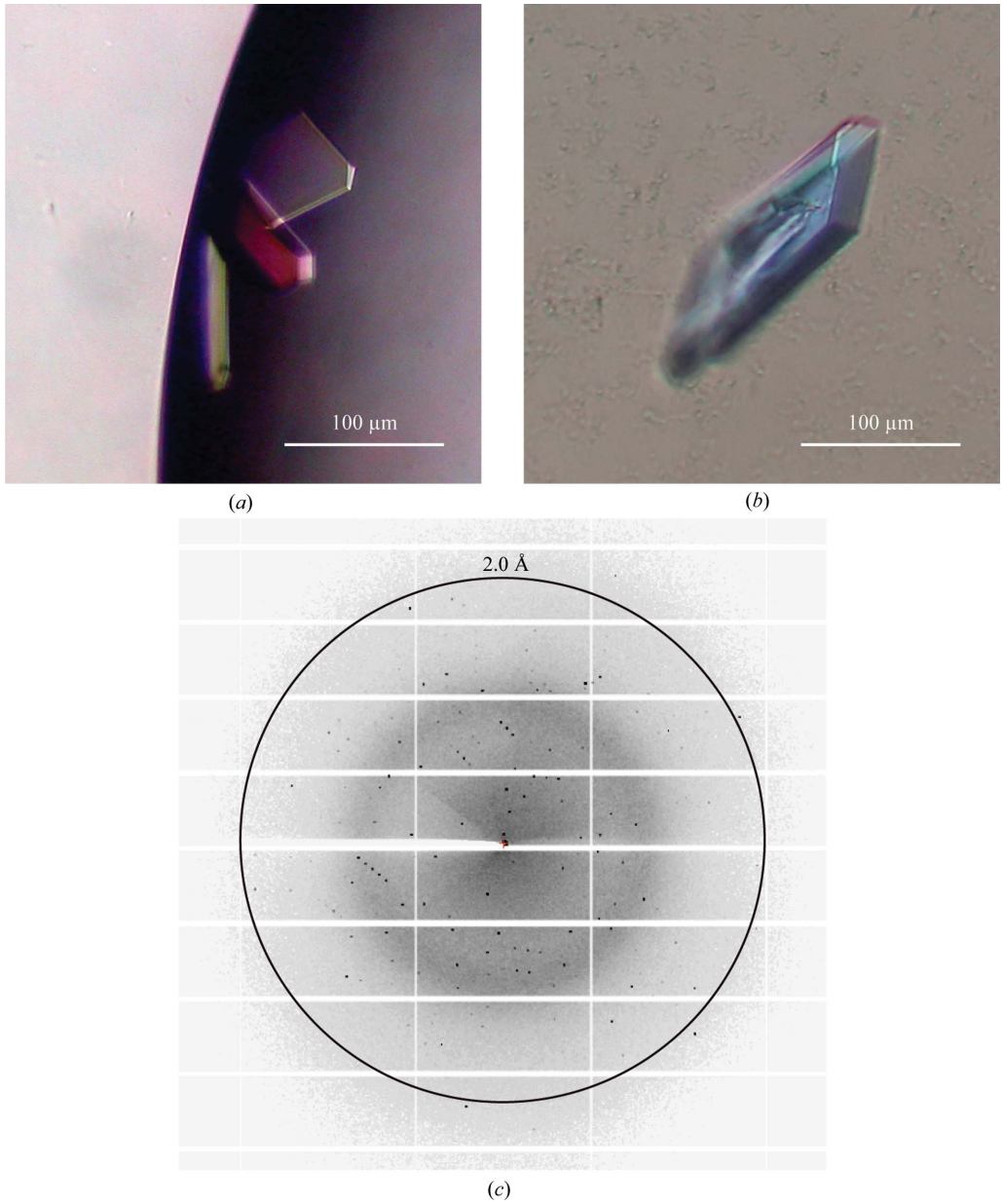

(*a*) (*b*) (*c*)

Figure 3
Crystals and X-ray diffraction image of the Enpp6 C393A/C412S mutant. (*a*) Crystals of the Enpp6 C393A/C412S mutant obtained by the initial screening. (*b*) Crystals of the Enpp6 C393A/C412S mutant obtained under the optimized conditions. (*c*) X-ray diffraction image of the Enpp6 C393A/C412S mutant.

Enpp6 has five conserved cysteine residues (Cys84, Cys142, Cys154, Cys393 and Cys412; Fig. 1). Mass-spectrometric analyses revealed that Cys142 and Cys154 of bovine Enpp6, which correspond to Cys142 and Cys154 of mouse Enpp6, respectively, form an intramolecular disulfide bond and that Cys414 of bovine Enpp6, which corresponds to Cys412 of mouse Enpp6, forms an intermolecular disulfide bond (Greiner-Tollersrud *et al.*, 2013). These observations suggested that Cys412 of mouse Enpp6 is involved in disulfide-mediated oligomerization. To examine the effects of these cysteine residues on oligomerization, we prepared three mutants of mouse Enpp6 (C84A, C393A and C412S). Western blotting analysis showed that the C412S mutant predominantly exists as a monomer (Fig. 2*d*), suggesting that Cys412 is involved in the disulfide-mediated dimerization. The Western blotting analysis further revealed that the expression levels of the C393A and C412S mutants were increased compared with that of the wild type (Fig. 2*d*). We thus expressed the C393A/C412S double mutant in HEK293T cells and purified it using P20.1-Sepharose. The C393A/C412S mutant predominantly eluted as a monomer from the gel-filtration column (Fig. 2*a*). The final yields of the wild type and C393A/C412S mutant of Enpp6 were 0.25 and 0.5 mg from 0.5 l culture, respectively. The C393A/C412S mutant displayed phosphodiesterase activity comparable to that of the wild type (data not shown), confirming that the C393A/C412S mutation does not affect the Enpp6 function. Thus, we used the C393A/C412S mutant for crystallization trials.

3.2. Crystallization

After the initial screening, we obtained clustered crystals under condition No. 8 of The PACT Screen [0.2 *M* ammonium chloride, 0.1 *M* sodium acetate pH 5.0, 20%(*w*/*v*) PEG 6000; Fig. 3*a*]. The conditions were optimized by adjusting the pH, the concentration of PEG and the types of salt in the reservoir solution. We found that the addition of zinc sulfate into the reservoir enhanced the growth of single crystals. Finally, we obtained single crystals under crystallization conditions consisting of 0.2 *M* ammonium chloride, 0.1 *M* sodium acetate pH 4.5, 20%(*w*/*v*) PEG 6000, 0.2 m*M* zinc sulfate (Fig. 3*b*).

3.3. Data collection and preliminary crystallographic analysis

The crystal of the C393A/C412S mutant diffracted to 1.8 Å resolution (Fig. 3*c*) and belonged to space group *P*1, with unit-cell parameters $a = 63.7$, $b = 68.8$, $c = 69.7$ Å, $\alpha = 60.6$, $\beta = 87.0$, $\gamma = 68.1^\circ$. The data-collection statistics are summarized in Table 1. Assuming the presence of two protein molecules (48.5 kDa calculated from the amino-acid sequence) per asymmetric unit, the Matthews coefficient (V_M) was estimated to be 2.44 Å^3 Da^{-1}, with a solvent content of 49.5% (Matthews, 1968). Molecular replacement was performed using the catalytic domain of mouse Enpp1 (PDB entry 4gtw; 32% sequence identity; Kato, Nishimasu, Okudaira *et al.*, 2012) as a search model, which provided a clear solution with a translation-function contrast value of 10.2. *REFMAC*5 (Murshudov *et al.*, 2011) was used for initial refinement, resulting in an *R* factor of 46.8% and an R_{free} of 50.0%. Further structural refinement is now in progress.

We thank the beamline staff at PXI of the Swiss Light Source for technical help during data collection. This work was supported by the Platform for Drug Discovery, Informatics and Structural Life Science from the Ministry of Education, Culture, Sports, Science and Technology, Japan. This work was supported by grants to ON from the Japan Society for the Promotion of Science (JSPS) through its 'Funding Program for World-Leading Innovative R&D on Science and Technology (FIRST program)' and the Core Research for Evolutional Science and Technology (CREST) Program 'The Creation of Basic Medical Technologies to Clarify and Control the Mechanisms Underlying Chronic Inflammation' of Japan Science and Technology Agency (JST), by Grants-in-Aid for Scientific Research (A) from MEXT to HN and by the scientific research projects 'Machinery of bioactive lipids in homeostasis and diseases' and 'Regulation of signal transduction by post-translational modifications and its pathogenic dysregulation' from the Ministry of Education, Culture, Sports, Science and Technology of Japan to ON.

Table 1
Data-collection statistics for Enpp6 C393A/C412S.

Values in parentheses are for the outer shell.

Beamline	PXI, SLS
Wavelength (Å)	1.278
Crystal-to-detector distance (mm)	180
Total oscillation range (°)	360
Oscillation range per image (°)	0.1
Exposure time per image (s)	0.1
Space group	*P*1
Unit-cell parameters (Å, °)	$a = 63.7$, $b = 68.8$, $c = 69.7$, $\alpha = 60.6$, $\beta = 87.0$, $\gamma = 68.1$
Resolution (Å)	50.0–1.8 (1.91–1.80)
Total reflections	290212
Unique reflections	81807
Multiplicity	3.54 (3.28)
Completeness (%)	93.6 (88.5)
$\langle I/\sigma(I)\rangle$	12.8 (2.06)
R_{merge}†	0.058 (0.543)
Mosaicity (°)	0.076
Overall *B* factor from Wilson plot (Å^2)	26.5

† $R_{merge} = \sum_{hkl}\sum_i |I_i(hkl) - \langle I(hkl)\rangle| / \sum_{hkl}\sum_i I_i(hkl)$, where $I_i(hkl)$ is the *i*th observation of reflection *hkl* and $\langle I(hkl)\rangle$ is the weighted average intensity for all observations of reflection *hkl*.

References

Albright, R. A., Chang, W. C., Robert, D., Ornstein, D. L., Cao, W., Liu, L., Redick, M. E., Young, J. I., De La Cruz, E. M. & Braddock, D. T. (2012). *Blood*, **120**, 4432–4440.
Albright, R. A., Ornstein, D. L., Cao, W., Chang, W. C., Robert, D., Tehan, M., Hoyer, D., Liu, L., Stabach, P., Yang, G., De La Cruz, E. M. & Braddock, D. T. (2013). *J. Biol. Chem.* **289**, 3294–3306.
Gouet, P., Robert, X. & Courcelle, E. (2003). *Nucleic Acids Res.* **31**, 3320–3323.
Greiner-Tollersrud, L., Berg, T., Stensland, H. M. F. R., Evjen, G. & Greiner-Tollersrud, O. K. (2013). *Neurochem. Res.* **38**, 300–310.
Hausmann, J. *et al.* (2011). *Nature Struct. Mol. Biol.* **18**, 198–204.
Hessle, L., Johnson, K. A., Anderson, H. C., Narisawa, S., Sali, A., Goding, J. W., Terkeltaub, R. & Millan, J. L. (2002). *Proc. Natl Acad. Sci. USA*, **99**, 9445–9449.
Jansen, S., Perrakis, A., Ulens, C., Winkler, C., Andries, M., Joosten, R. P., Van Acker, M., Luyten, F. P., Moolenaar, W. H. & Bollen, M. (2012). *Structure*, **20**, 1948–1959.
Kabsch, W. (2010). *Acta Cryst.* D**66**, 125–132.
Kato, K., Nishimasu, H., Mihara, E., Ishitani, R., Takagi, J., Aoki, J. & Nureki, O. (2012). *Acta Cryst.* F**68**, 778–782.
Kato, K., Nishimasu, H., Okudaira, S., Mihara, E., Ishitani, R., Takagi, J., Aoki, J. & Nureki, O. (2012). *Proc. Natl Acad. Sci. USA*, **109**, 16876–16881.
Korekane, H., Park, J. Y., Matsumoto, A., Nakajima, K., Takamatsu, S., Ohtsubo, K., Miyamoto, Y., Hanashima, S., Kanekiyo, K., Kitazume, S., Yamaguchi, Y., Matsuo, I. & Taniguchi, N. (2013). *J. Biol. Chem.* **288**, 27912–27926.
Larkin, M. A., Blackshields, G., Brown, N. P., Chenna, R., McGettigan, P. A., McWilliam, H., Valentin, F., Wallace, I. M., Wilm, A., Lopez, R., Thompson, J. D., Gibson, T. J. & Higgins, D. G. (2007). *Bioinformatics*, **23**, 2947–2948.
Matthews, B. W. (1968). *J. Mol. Biol.* **33**, 491–497.
Murshudov, G. N., Skubák, P., Lebedev, A. A., Pannu, N. S., Steiner, R. A., Nicholls, R. A., Winn, M. D., Long, F. & Vagin, A. A. (2011). *Acta Cryst.* D**67**, 355–367.

Nishimasu, H., Okudaira, S., Hama, K., Mihara, E., Dohmae, N., Inoue, A., Ishitani, R., Takagi, J., Aoki, J. & Nureki, O. (2011). *Nature Struct. Mol. Biol.* **18**, 205–212.
Sakagami, H., Aoki, J., Natori, Y., Nishikawa, K., Kakehi, Y., Natori, Y. & Arai, H. (2005). *J. Biol. Chem.* **280**, 23084–23093.
Stefan, C., Jansen, S. & Bollen, M. (2005). *Trends Biochem. Sci.* **30**, 542–550.
Tabata, S., Nampo, M., Mihara, E., Tamura-Kawakami, K., Fujii, I. & Takagi, J. (2010). *J. Proteomics*, **73**, 1777–1785.
Umezu-Goto, M., Kishi, Y., Taira, A., Hama, K., Dohmae, N., Takio, K., Yamori, T., Mills, G. B., Inoue, K., Aoki, J. & Arai, H. (2002). *J. Cell Biol.* **158**, 227–233.
Vagin, A. & Teplyakov, A. (2010). *Acta Cryst.* D**66**, 22–25.
Vries, R. P. de, de Vries, E., Bosch, B. J., de Groot, R. J., Rottier, P. J. M. & de Haan, C. A. M. (2010). *Virology*, **403**, 17–25.